UDC 621.3.013 https://doi.org/10.20998/2074-272X.2024.4.03

B.I. Kuznetsov, T.B. Nikitina, I.V. Bovdui, K.V. Chunikhin, V.V. Kolomiets, B.B. Kobylianskyi

The method for design of electromagnetic hybrid active-passive shielding by overhead power lines magnetic field

Aim. *Development of the method for designing electromagnetic hybrid active-passive shield, consisting from active and multy-circuit passive parts, which is characterized by increased effectiveness of reducing the industrial frequency magnetic field created by two-circuit overhead power lines in residential buildings.* ***Methodology****. The designing problem of electromagnetic hybrid active-passive shield including robust system of active shielding and multy-circuit passive shield of initial magnetic field comes down to a solution of the multy-criteria two-player zero-sum antagonistic game. The game payoff vector calculated based on the finite element calculations system COMSOL Muliphysics. The game solution calculated based on the particles multyswarm optimization algorithms.* ***Results.*** *During the design of the electromagnetic hybrid active-passive shield the coordinates of the spatial arrangement of 11 circuits passive shield and the coordinates of the spatial location of one compensation winding, as well as the current and phase in this winding of the active shielding system are calculated. The results of theoretical and experimental studies of hybrid active and multy-circuit passive shield by magnetic field in residential building from two-circuit power transmission line with a «Barrel» type arrangement of wires presented.* ***Originality****. For the first time the method for designing hybrid active and multy-circuit passive shield, consisting from active and multy-circuit passive parts, which is characterized by increased effectiveness of reducing the magnetic field of industrial frequency created by two-circuit overhead power lines in residential buildings is developed.* ***Practical value****. Based on results of calculated study the shielding efficiency of the initial magnetic field what is confirmed by experimental studies determined that shielding factors whith only multy-circuit passive shield is more 1.2 units, whith only active shield is more 4 units and with electromagnetic hybrid active-passive shield is more 6.2 units. It is shown the possibility to reduce the level of magnetic field induction in residential building from two-circuit power transmission line with a «Barrel» type arrangement of wires by means of electromagnetic hybrid active shielding with single compensating winding and multy-circuit passive shielding with 11 circuit passive shield to 0.5 μT level safe for the population.* References 51, figures 17.

Key words: **overhead power line, magnetic field, electromagnetic hybrid active-passive shield, computer simulation, experimental research.**

Мета*. Розробка методу проектування електромагнітного гібридного активно-пасивного екрану, який складається з активної та багатоконтурної пасивної частин, та характеризується підвищеною ефективністю зниження магнітного поля промислової частоти, що генерується дволанцюговими повітряними лініями електропередачі в житлових будинках.* ***Методологія.*** *Задача проектування електромагнітного гібридного активно-пасивного екрану, яка включає розробку робастної системи активного екранування та багатоконтурного пасивного екрану вихідного магнітного поля, зводиться до вирішення багатокритеріальної антагоністичної гри двох гравців з нульовою сумою. Вектор виграшів гри розраховується з використанням кінцево-елементної системи обчислень COMSOL Muliphysics. Рішення гри розраховується на основі алгоритмів оптимізації мультироїв частинок.* ***Результати.*** *При проектуванні електромагнітного гібридного активно-пасивного екрану були розраховані координати просторового розташування 11 контурів пасивного екрану і координати просторового розташування однієї компенсаційної обмотки, а також струм і фаза в цій обмотці системи активного екранування. Наведено результати теоретичних та експериментальних досліджень електромагнітного гібридного активно-пасивного екрану магнітного поля в житловому будинку від дволанцюгової лінії електропередач із розташуванням проводів типу «бочка».* ***Оригінальність.*** *Вперше розроблено метод проектування електромагнітного гібридного активно-пасивного екрану, який складається з активної та багатоконтурної пасивної частин, та характеризується підвищеною ефективністю зниження рівня магнітного поля промислової частоти, яке генерується дволанцюговими повітряними лініями електропередачі в житлових будинках.* ***Практична цінність****. За результатами розрахункових досліджень ефективності екранування вихідного магнітного поля, які підтверджені експериментальними дослідженнями, встановлено, що коефіцієнт екранування тільки багатоконтурним пасивним екраном становить більше 1,2 одиниць, а тільки з активним екраном становить більше 4 одиниць, і при використанні електромагнітного гібридного активно-пасивного екрану становить більше 6,2 одиниці. Показана можливість зниження рівня індукції магнітного поля в житловому будинку від дволанцюгової лінії електропередачі з розташуванням проводів типу «бочка» за допомогою гібридного активного екрану з однією компенсуючою обмоткою та багатоконтурного пасивного екрану з 11 контурами до безпечного для населення рівня в 0,5 μТ.* Бібл. 51, рис. 17.

Ключові слова: **повітряна лінія електропередачі, магнітне поле, електромагнітний гібридний активно-пасивний екран, комп'ютерне моделювання, експериментальні дослідження.**

Introduction. Overhead power lines are the main source of power frequency magnetic field (MF). The effect of prolonged exposure of people to a power frequency MF increase in the likelihood of cancer [1–3]. The standards for the power frequency MF being tightened for long-term safe residence of the population in residential buildings located near power lines. Decrease in the initial MF by a factor of 2–4 is required [4–7]. Active and passive shielding of the initial MF usually used for reduction of power frequency MF [4–10].

Active shielding requires the use of external power supplies to supply currents appropriate magnitude and phase to the reduction system opposite to the original MF to provide the desired reduction effect, and as such, is capable of providing a high reduction in the original MF [11–15]. However, this requires a complex suppression system; since in addition to the MF sensors, it is necessary to install expensive equipment, such as power supplies, and a monitoring system to continuously adjust the supplied current to achieve the required suppression. All this makes this solution much more expensive than passive methods.

With passive shielding, MF weakening is achieved, since the mitigation system acts in response to the initial MF generated by the source according to Faraday's law

and induces currents that generate a new MF that compensates for the original one [16–20]. To increase the shielding efficiency of the initial MF, multy-circuit passive shields are often used [21, 22]. Passive shield have a significantly lower shielding factor, so passive screens are often used as a complement to active screens [23–25].

The aim of the work is to develop the method for designing electromagnetic hybrid active-passive shield, consisting from active and multy-circuit passive parts, to improve the effectiveness of reduction of industrial frequency MF created by two-circuit overhead power lines in residential buildings.

Problem statement. First, consider the design of the mathematical model of the initial MF generated by the power transmission line. We set the currents amplitude $\boldsymbol{A_i}$ and phases $\boldsymbol{\varphi_i}$ of power frequency ω of wires currents power lines. Then we set wires currents in power lines in a complex form

$$\boldsymbol{I_i}(t) = \boldsymbol{A_i} \exp j(\omega t + \boldsymbol{\varphi_i}). \quad (1)$$

To assess the impact of the MF of power lines on the environment, most calculations were performed based on the Biot-Savart-Laplace law [6] for elementary current

$$\mathrm{d}\,\boldsymbol{B_l}(Q_i,t) = \frac{\mu\mu_0 i_l(t)}{4\pi R^3}(\mathrm{d}\,\boldsymbol{l}_l \times \boldsymbol{R}_l), \quad (2)$$

where the vector $\boldsymbol{R}_l$ is directed from an elementary segment $\mathrm{d}\boldsymbol{l}_l$ with a total current $\boldsymbol{i_l}(t)$ to the observation point Q_i, μ_0 is the vacuum magnetic permeability.

Then the total MF vector is equal to:

$$\boldsymbol{B_l}(Q_i,t) = \frac{\mu\mu_0 \boldsymbol{i_l}(t)}{4\pi}\int_L \frac{(\mathrm{d}\boldsymbol{l}_l \times \boldsymbol{R}_l)}{R^3}. \quad (3)$$

This formula is widely used to calculate the MF of air power transmission lines instead of Maxwell's system of equations.

Let us introduce the vector $\boldsymbol{\delta}$ of the uncertainty parameters of the problem of designing a combined shield, the components of which are inaccurate knowledge of the currents and phases in the wires of the power transmission line, as well as other parameters of the electromagnetic hybrid active-passive shield, which, firstly, are initially known inaccurately and, secondly, may change during the operation of the system [26–28].

Then the vector $\boldsymbol{B_L}(Q_i,\boldsymbol{\delta},t)$ of the initial MF generated by all power lines wires $\boldsymbol{B_{Li}}(Q_i,\boldsymbol{\delta},t)$ in point Q_i of the shielding space calculated based Biot-Savart's law [6]

$$\boldsymbol{B_L}(Q_i,\boldsymbol{\delta},t) = \sum \boldsymbol{B_l}(Q_i,\boldsymbol{\delta},t). \quad (4)$$

Now, consider the design of the mathematical model of the MF generated by compensating windings of active shielding. We set the vector $\boldsymbol{X_a}$ of initial geometric values of the dimensions of the compensating windings of active shielding, as well as the currents amplitude $\boldsymbol{A_{ai}}$ and phases $\boldsymbol{\varphi_{ai}}$ in the compensating windings [29–33]. We set the currents in the compensating windings wires in a complex form

$$\boldsymbol{I_{ai}}(t) = \boldsymbol{A_{ai}} \exp j(\omega t + \varphi_{\boldsymbol{wi}}). \quad (5)$$

Then the vector $\boldsymbol{B_a}(Q_i,\boldsymbol{X_a},t)$ of the MF generated by all compensating windings wires of active shielding $\boldsymbol{B_{ai}}(Q_i,\boldsymbol{X_a},t)$ in point Q_i of the shielding space can also calculated based Biot-Savart's law [6]

$$\boldsymbol{B_a}(Q_i,\boldsymbol{X_a},t) = \sum \boldsymbol{B_{ai}}(Q_i,\boldsymbol{X_a},t) \quad (6)$$

Then the vector $\boldsymbol{B_{Ra}}(Q_i,\boldsymbol{X_a},\boldsymbol{\delta},t)$ of the resulting MF generated by power lines and only windings of the active shielding system calculated as sum

$$\boldsymbol{B_{Ra}}(Q_i,\boldsymbol{X_a},\boldsymbol{\delta},t) = \boldsymbol{B_L}(Q_i,\boldsymbol{\delta},t) + \boldsymbol{B_a}(Q_i,\boldsymbol{X_a},t) \quad (7)$$

Now, consider the design of the mathematical model of the MF generated by multy-circuit passive shield [35–37]. Let us set the vector $\boldsymbol{X_p}$ of initial values of the geometric dimensions, thickness and material of the multy-circuit passive loop shield. Then, for the given vector $\boldsymbol{B_{Ra}}(Q_i,\boldsymbol{X_a},\boldsymbol{\delta},t)$ of the resulting MF generated by power lines and only windings of the active shielding system and for values of the vector $\boldsymbol{X_p}$ of geometric dimensions of the passive loop shield, the magnetic flux $\boldsymbol{\Phi_l}(\boldsymbol{X_a},\boldsymbol{X_p},\boldsymbol{\delta},t)$ calculated

$$\boldsymbol{\Phi_l}(\boldsymbol{X_a},\boldsymbol{X_p},\boldsymbol{\delta},t) = \int_S \boldsymbol{B_{Ra}}(\boldsymbol{X_a},\boldsymbol{\delta},t)\mathrm{d}S. \quad (8)$$

The current $\boldsymbol{I_{Pl}}(\boldsymbol{X_a},\boldsymbol{X_p},\boldsymbol{\delta},t)$ in a complex form induced in the passive loop shield determined from Ohm law in integral form and Faraday law [6]:

$$\boldsymbol{I_{Pl}}(\boldsymbol{X_a},\boldsymbol{X_p},\boldsymbol{\delta},t) = -j\omega\boldsymbol{\Phi}(\boldsymbol{X_a},\boldsymbol{X_p},\boldsymbol{\delta},t)/\ldots \\ \ldots/(\boldsymbol{R_l}(\boldsymbol{X_p}) + j\omega\boldsymbol{L_l}(\boldsymbol{X_p})). \quad (9)$$

The active resistance $\boldsymbol{R_l}(\boldsymbol{X_p})$ and the self-inductance coefficient $\boldsymbol{L_l}(\boldsymbol{X_p})$ of the passive loop shield.

Then for the calculated currents $\boldsymbol{I_{Pl}}(\boldsymbol{X_a},\boldsymbol{X_p},\boldsymbol{\delta},t)$ in the passive loop screen [36–38] and their geometric dimensions given by the vector $\boldsymbol{X_p}$, on the basis of Biot-Savart's law, the vector $\boldsymbol{B_R}(Q_i,\boldsymbol{X_a},\boldsymbol{\delta},t)$ of the resulting MF calculated as sum the vector $\boldsymbol{B_L}(Q_i,\boldsymbol{\delta},t)$ generated by overhead power transmission lines, the vector $\boldsymbol{B_a}(Q_i,\boldsymbol{X_a},t)$ generated by all compensating windings wires of active shielding and the vector $\boldsymbol{B_p}(Q_i,\boldsymbol{X_a},\boldsymbol{X_p},\boldsymbol{\delta},t)$ generated by all loops of the passive shield at the point Q_i, similarly (7)

$$\boldsymbol{B_R}(Q_i,\boldsymbol{X_a},\boldsymbol{X_p},\boldsymbol{\delta},t) = \boldsymbol{B_L}(Q_i,\boldsymbol{\delta},t) + \ldots \\ \ldots + \boldsymbol{B_a}(Q_i,\boldsymbol{X_a},t) + \boldsymbol{B_p}(Q_i,\boldsymbol{X_a},\boldsymbol{X_p},\boldsymbol{\delta},t). \quad (10)$$

Solution method. We introduce the vector $\boldsymbol{X}$ of the desired parameters of the problem of designing a combined shield, the components of which are the vector $\boldsymbol{X_a}$ values of the geometric dimensions of the compensation windings, as well as the currents $\boldsymbol{A_{wi}}$ and phases $\boldsymbol{\varphi_{wi}}$ in the compensation windings, as well as the vector $\boldsymbol{X_p}$ of geometric dimensions, thickness and material of the passive loop shield [39, 40].

Then for the given initial values of the vector $\boldsymbol{X}$ of the desired parameters and the vector $\boldsymbol{\delta}$ of the uncertainty parameters of the combined screen design problem, the value $\boldsymbol{B_R}(\boldsymbol{X},\boldsymbol{\delta},P_i)$ effective value of induction of the resulting MF $\boldsymbol{B_R}(Q_i,\boldsymbol{X_a},\boldsymbol{X_p},\boldsymbol{\delta},t)$ at the point Q_i of the shielding space calculated based on the finite element calculations system COMSOL Multiphysics. Then the problem of designing a passive screen is reduced to computing the solution of the vector game

$$\boldsymbol{B_R}(\boldsymbol{X},\boldsymbol{\delta}) = \langle \boldsymbol{B_R}(\boldsymbol{X},\boldsymbol{\delta},P_1)\rangle. \quad (11)$$

The components of the game payoff vector $\boldsymbol{B_R}(\boldsymbol{X},\boldsymbol{\delta},P_i)$ are the effective values of the induction of the resulting MF at all considered points Q_i in the shielding space.

In this vector game it is necessary to find the minimum of the game payoff vector (11) by the vector $\boldsymbol{X}$, but the maximum of the same game payoff vector by the vector $\boldsymbol{\delta}$.

At the same time, naturally, it is necessary to take into account constraints [41] on the vector $\boldsymbol{X}$ desired parameters of a combined shield in the form of vector inequality and, possibly, vector equality

$$\boldsymbol{G}(\boldsymbol{X}) \le \boldsymbol{G}_{max}, \quad \boldsymbol{H}(\boldsymbol{X}) = 0. \qquad (12)$$

Note that the components of the vector game (11) and vector constraints (12) are the nonlinear functions of the vector of the required parameters [42–45] and calculated based on the calculations system COMSOL Multiphysics.

Solution algorithm. Let us consider an algorithm for solving on a computer the formulated multyobjective optimization problem (11) with constraints (12). To find a unique solution to the problem of multycriteria optimization from the Pareto set of optimal solutions, in addition to the vector optimization criterion (11) and constraints (12), it is also necessary to have information about the binary preference relations of local solutions relative to each other [46–48].

To find such a single optimal solution, it is first necessary to develop an algorithm for constructing the entire area of Pareto-optimal solutions. Then, based on the analysis of the entire set of possible optimal solutions to the original problem of multycriteria optimization, narrow the range of solutions under consideration and, consequently, reduce the complexity of the decision maker in choosing the only option for the optimal solution.

A feature of the considered problem of finding a local minimum at one point in the space under consideration is multy-extremality, so that the considered area of possible solutions contains local minima and maxima. This is due to the fact that when minimizing the level of induction of the resulting MF in one current of the search space, the induction at another point increases due to undercompensation or overcompensation of the initial MF. Therefore, to solve the considered multycriteria problem, it is advisable to use the algorithms of stochastic multy-agent optimization [48–50].

Consider an algorithm for finding a set of Pareto-optimal solutions to multyobjective non-linear programming problems based on stochastic multy-agent optimization – PSO algorithms based on the idea of a collective mind of a swarm of particles, based on algorithms for finding the globally optimal value $y_j^*(t)$ – gbest PSO found by all particles swarm, and the locally optimal value $y_{ij}(t)$ – lbest PSO found by one swarm particle [48–50].

At present, the use of stochastic multy-agent optimization methods for solving multycriteria optimization problems causes certain difficulties, but this direction continues to be intensively developed using various heuristic techniques. Consider a stochastic multy-agent optimization algorithm for solving the original multycriteria problem of nonlinear programming (11) with constraints (12) based on a set of swarms j of particles i, the number of which is equal to the number of components of the vector optimization criterion (11).

In the simplest algorithm for calculating the optimal position $x_{ij}(t)$ and speed $v_{ij}(t)$ of the movement of particle i swarm j, the movement speeds $v_{ij}(t)$change according to linear laws. However, recently, to increase the speed of finding a global solution, special non-linear algorithms of stochastic multy-agent optimization have become widespread. One of such algorithms is an algorithm in which the Heaviside function H is used to switch the motion of a particle, respectively, from the local $y_{ij}(t)$ to the global $y_j^*(t)$ optimum. Parameters of switching the cognitive p_{1j} and social p_{2j} components of the speed of particle movement in accordance with the local and global optimum; random numbers $\varepsilon_{1j}(t)$ and $\varepsilon_{2j}(t)$ determine the parameters of switching the movement of the particle according to the local and global optimum. If $p_{1j} < \varepsilon_{1j}(t)$ and $p_{2j} < \varepsilon_{2j}(t)$, then the speed of movement of particle i swarm j does not change at the step t and the particle moves in the same direction as in the previous optimization step. In this algorithm, the motion of particle i swarm j described by the following expressions

$$\begin{aligned} v_{ij}(t+1) = w_j v_{ij}(t) + c_{1j} r_{1j}(t) H\left(p_{1j} - \varepsilon_{1j}(t)\right) \times \dots \\ \dots \times \left[y_{ij}(t) - x_{ij}(t)\right] + c_{2j} r_{2j}(t) H\left(p_{2j} - \varepsilon_{2j}(t)\right) \times \dots \\ \dots \times \left[y_j^*(t) - x_{ij}(t)\right], \end{aligned} \qquad (13)$$

$$x_{ij}(t+1) = x_{ij}(t) + v_{ij}(t+1), \qquad (14)$$

where c_1, c_2 are positive constants that determine the weights of the cognitive and social components of the speed of particle movement; $r_{1j}(t)$, $r_{2j}(t)$ are random numbers from the range [0, 1], which determine the stochastic component of the particle's speed.

With the multycriteria optimization of the vector criterion (11), with the help of separate swarms, the optimization problems of scalar criteria, which are components, are solved. In order to find a global solution to the original multycriteria problem.

In the process of searching for a global solution to the original multycriteria problem (11), individual swarms exchange information with each other in the course of searching for optimal solutions to local criteria. Information about the global optimum obtained by the particles of another swarm is used to calculate the speed of movement of the particles of the other swarm, which makes it possible to calculate all potential Pareto-optimal solutions.

At each step t of the movement of particle i swarm j, the advantages functions $y_{ij}(t)$ of local solutions obtained by all swarms y_j^* are used. The solution $X_j^*(t)$ obtained during the optimization of the objective function $B(X(t),P_j)$ using the swarm j is better than the solution $X_k^*(t)$ obtained during the optimization of the objective function $B(X(t),P_k)$ using the swarm k, i.e. $X_j^*(t) \succ X_k^*(t)$, if the condition is fulfilled

$$\max_{i=1,m} B\left(P_i, X_j^*(t)\right) < \max_{i=1,m} B\left(P_i, X_k^*(t)\right). \qquad (15)$$

The global solution $X_k^*(t)$ obtained by the swarm k used as the global optimal solution $X_j^*(t)$ of the swarm j, which is better in relation to the global solution $X_k^*(t)$ of the swarm k on the basis of the preference relationship (15).

The main idea of successively narrowing of Pareto-optimal solutions area of trade-offs – all that cannot be chosen according to the available information about the preference are sequentially removed from the initial set of

possible solutions based on information about the relative importance of local solutions. The deletion is carried out until a globally optimal solution is obtained [51].

Simulation results. Let us consider the results of the design of electromagnetic hybrid active-passive shielding by overhead power lines MF generated by a double-circuit power line in a residential building. During the design of the electromagnetic hybrid active-passive shield, the coordinates of the spatial arrangement of 11 circuits passive screens were calculated. In addition, the coordinates of the spatial location of one compensation winding, as well as the current and phase in this winding of the active shielding system, were calculated.

Note that, unlike the works [21, 22], in this work the coordinates of the spatial arrangement of the contours of the multyloop passive screen calculated in the course of solving the multy-criteria two-player antagonistic game (10) with restrictions (11) and electromagnetic hybrid active-passive shield used to screen the initial MF.

The layout of the power transmission line, the winding of the active screen and 11 circuits passive screen shown in Fig. 1.

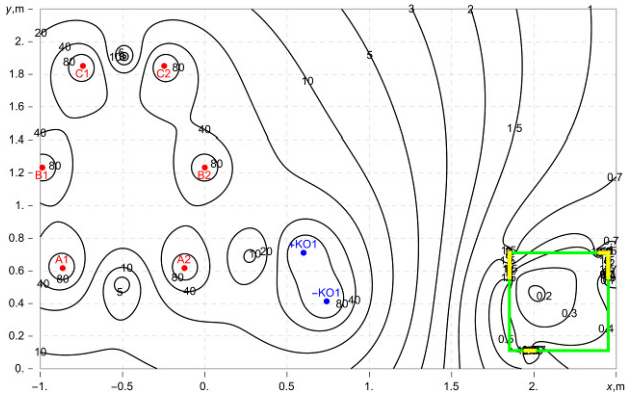

Fig. 1. The layout of the power transmission line, the winding of the active screen and 11 circuits of the passive screen

Figure 2 shows the distribution of the calculated initial MF induction. Initial MF induction changes from 2.2 μT to 1.4 μT. MF induction level in the central part of the shielding space is 1.75 μT.

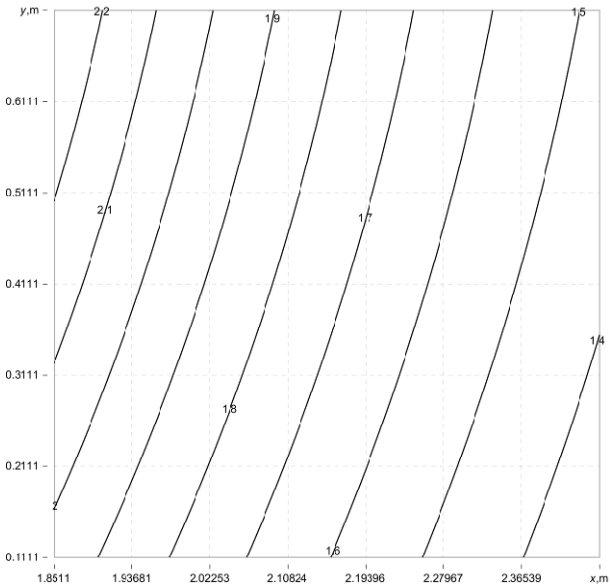

Fig. 2. The distribution of the calculated initial MF induction

Figure 3 shows the distribution of the calculated resulting MF induction with only multy-circuit passive shield. The coordinates of the spatial arrangement of 11 multy-circuit passive screens were calculated during the design of the hybrid multy-circuits passive and active shielding.

The resulting MF induction with only multy-circuit passive screen changes from 2 μT to 1.35 μT. The MF level in the central part of the shielding space is 1.35 μT.

The calculated shielding factor maximum value of resulting MF whith only multy-circuit passive shield in the central part of the screening space is more 1.29 units.

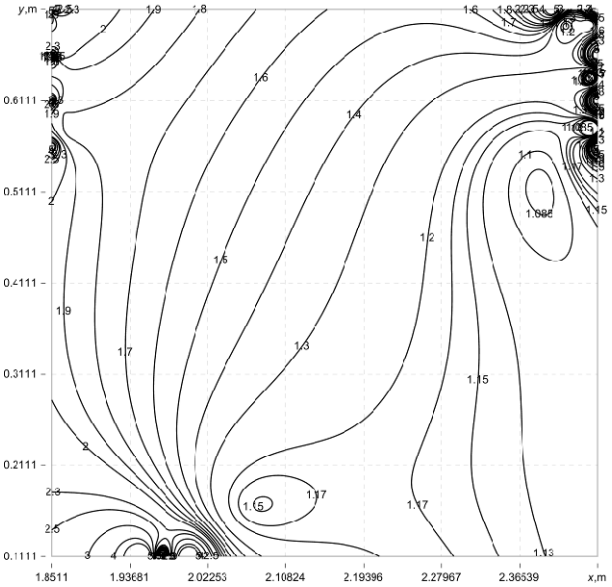

Fig. 3. The distribution of the calculated resulting MF induction with only multy-circuit passive shield

Figure 4 shows the distribution of the calculated resulting MF induction with only active shield.

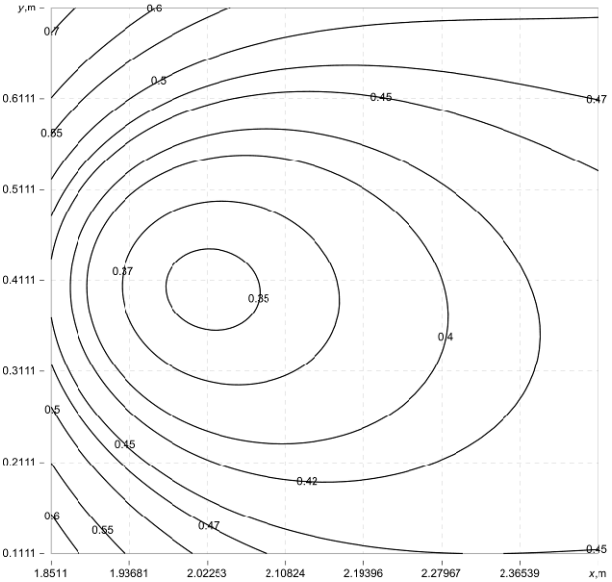

Fig. 4. The distribution of the calculated resulting MF induction with only active shield

The resulting MF induction with only active screen changes from 0.7 μT to 0.35 μT. The MF level in the central part of the shielding space is 0.35 μT.

The calculated shielding factor maximum value of resulting MF with only active shield in the central part of the screening space is more then 5 units.

Figure 5 shows the distribution of the calculated resulting MF induction with electromagnetic hybrid active-passive shield.

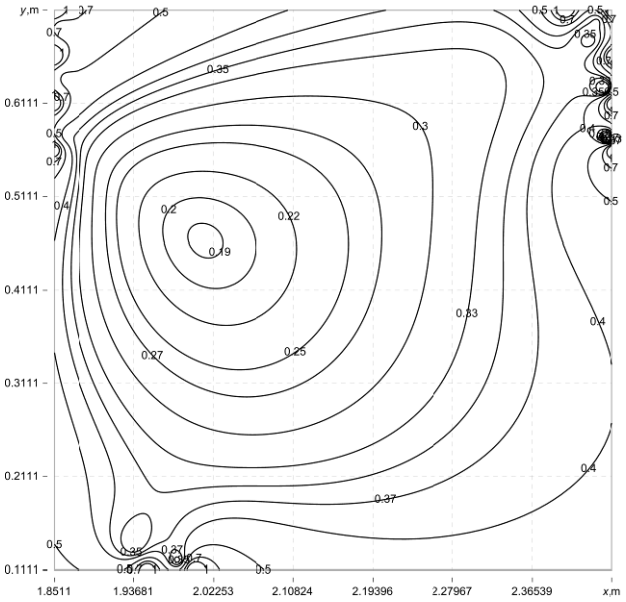

Fig. 5. The distribution of the calculated resulting MF induction with electromagnetic hybrid active-passive shield

The resulting MF induction with electromagnetic hybrid active-passive shield changes from 0.7 μT to 0.19 μT. The MF level in the central part of the shielding space is 0.19 μT.

The calculated shielding factor maximum value of resulting MF with only active shield in the central part of the screening space is more then 9.21 units.

Thus, the use of electromagnetic hybrid active-passive shield makes it possible to increase the screening factor of the active screen by 1.84 times.

Note that the product of shielding factors with only a multy-circuit passive screen of 1.29 and a shielding factor with only an active screen of 5 gives a value of 6.45, while the shielding factor with a electromagnetic hybrid active-passive shield is 9.21. Thus, the simultaneous use of active and multy-circuit passive screens leads to an increase in the screening factor by 1.42 times.

In addition, the use of electromagnetic hybrid active-passive shield makes it possible to reduce the level of the initial MF in a much larger area of the screening space compared to using only the active screen.

Results of experimental studies. Let us now consider the results of experimental studies of the electromagnetic hybrid active-passive shield.

Figure 6 shows the compensation winding and multy-circuit passive shield of the experimental setup.

Figure 7 shows multy-circuit passive shield and the control system of the experimental setup of multy-circuit passive and active shielding.

Figure 8 shows the experimental distribution of the initial and resulting MF induction with only multy-circuit passive shield.

Figure 9 shows the experimental shielding factor of resulting MF whith only multy-circuit passive shield.

The experimental shielding factor maximum value of resulting MF whith only multy-circuit passive shield is more then 1.2 units.

Fig. 6. The compensation winding and multy-circuit passive shield of the experimental setup

Fig. 7. The multy-circuit passive shield and the control system of the experimental setup of multy-circuit passive and active shielding

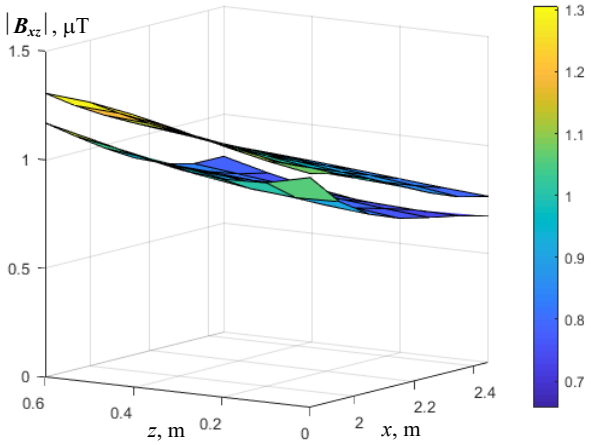

Fig. 8. The experimental distribution of the initial and resulting MF induction with only multy-circuit passive shield

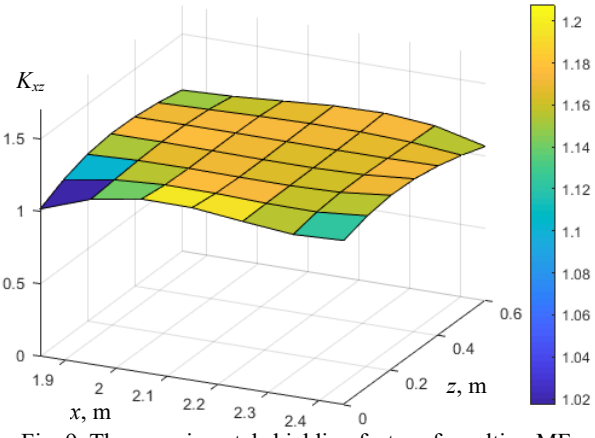

Fig. 9. The experimental shielding factor of resulting MF whith only multy-circuit passive shield

Figure 10 shows the experimental spatio-temporal characteristic of the resulting MF with only multy-circuit passive shield.

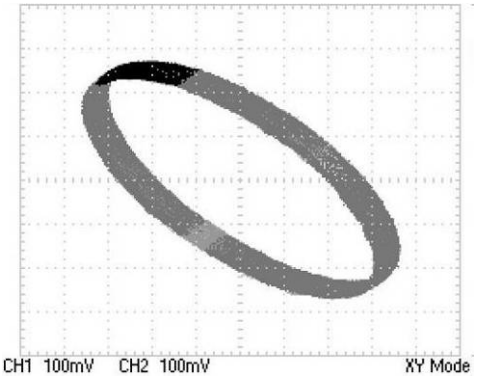

Fig. 10. The experimental spatio-temporal characteristic of the resulting MF with only multy-circuit passive shield

The experimental spatio-temporal characteristic of the resulting MF with only multy-circuit passive shield is about 1.2 times less than the spatio-temporal characteristic of the initial MF.

Figure 11 shows the experimental distribution of the initial and resulting MF induction with only active shield.

Figure 12 shows the experimental shielding factor of resulting MF whith only active shield.

The experimental shielding factor maximum value of resulting MF whith only active shield is more then 5 units.

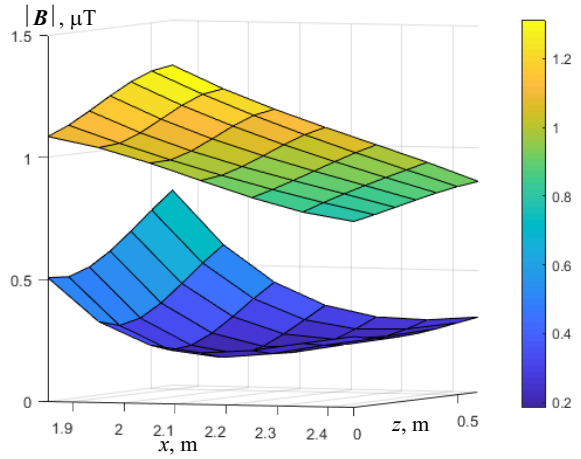

Fig. 11. The experimental distribution of the initial and resulting MF induction with only active shield

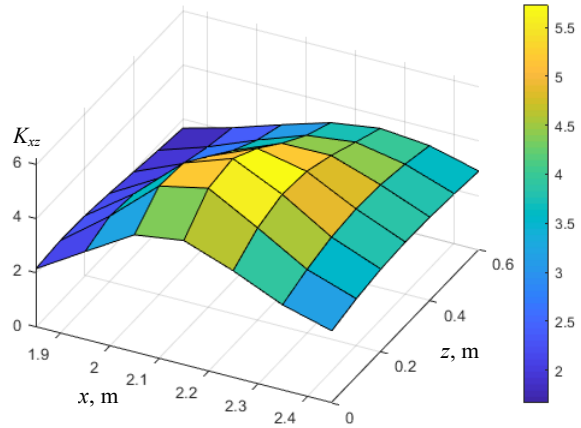

Fig. 12. The experimental shielding factor of resulting MF whith only active shield

Figure 13 shows the experimentally measured spatio-temporal characteristic of the MF generated by only one compensating winding of the active shielding system.

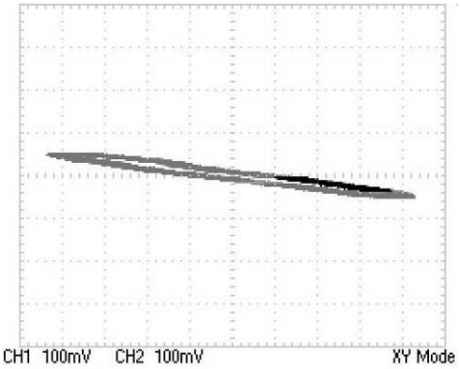

Fig. 13 Experimentally measured spatio-temporal characteristic of the MF generated by only one compensating winding of the active shielding system

This characteristic is practically a straight line parallel to the major axis of the ellipse of the experimentally measured spatiotemporal characteristic of the initial MF. Note that with the help of such an active screening system, the large axis of the spatiotemporal characteristic of the initial MF compensated, which determines the high value of the screening factor. In this case, the experimentally measured spatio-temporal characteristic of the resulting MF is a small cloud due to the noise of measurements of the MF components.

Figure 14 shows the experimental distribution of the initial and resulting MF induction with electromagnetic hybrid active-passive shield.

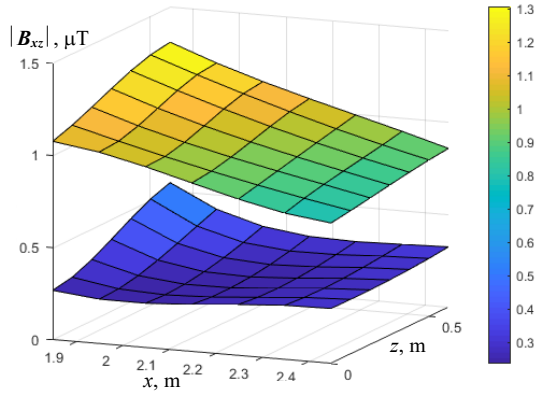

Fig. 14. The experimental distribution of the initial and resulting MF induction with electromagnetic hybrid active-passive shield

When using electromagnetic hybrid active-passive shield the level of the resulting MF is significantly lower in the entire shielding space than when using only the active shield.

Figure 15 shows the experimental shielding factor of resulting MF with electromagnetic hybrid active-passive shield.

The maximum value of the experimental shielding factor of the MF when using electromagnetic hybrid active-passive shield is more than 4.2 units. The main advantage of the hybrid multy-circuit passive and active shield is the significantly lower level of the resulting MF induction over the entire shielding space by a factor of two or more compared to the active shield.

Consider one more setting of the active screening system when using a hybrid screen. Figure 16 shows the experimental distribution of the initial and resulting MF induction with electromagnetic hybrid active-passive shield for another setting of the active shielding system.

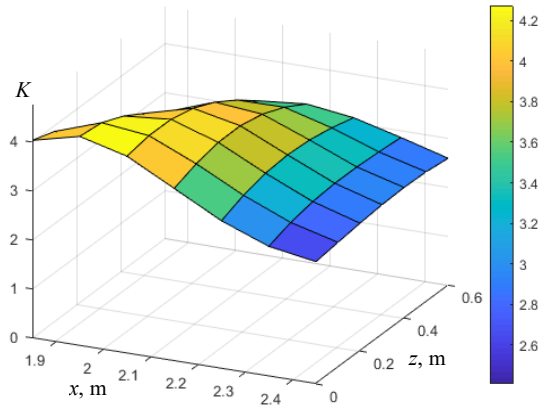

Fig. 15. The experimental shielding factor of resulting MF with electromagnetic hybrid active-passive shield

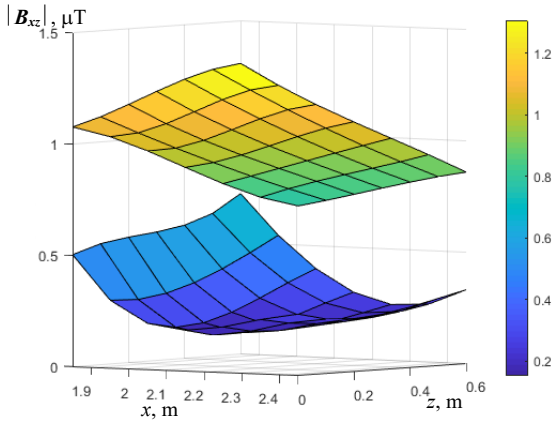

Fig. 16. The experimental distribution of the initial and resulting MF induction with electromagnetic hybrid active-passive shield for another setting of the active shielding system

Figure 17 shows the experimental shielding factor of resulting MF with electromagnetic hybrid active-passive shield for another setting of the active shielding system.

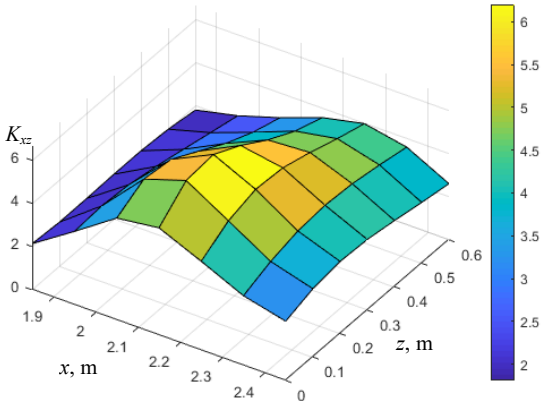

Fig. 17. The experimental shielding factor of resulting MF with electromagnetic hybrid active-passive shield for another setting of the active shielding system

For sush another setting of the active shielding system the maximum value of the experimental shielding factor of the MF when using electromagnetic hybrid active-passive shield is more 6.2 units, wich is more 1.47 times more than with the previously considered setting of the active shielding system. However, at the same time, at the edges of the shielding space, a significantly lower shielding efficiency is realized – more 1.7 times compared to the previously considered setting of the active shielding system.

Conclusions.

1. For the first time the method for designing electromagnetic hybrid active-passive shield, consisting from active and multy-circuit passive parts, which is characterized by increased effectiveness of reducing the industrial frequency magnetic field created by two-circuit overhead power lines in residential buildings was developed.

2. The problem of design of electromagnetic hybrid active-passive shield solved based on the multy-criteria two-player antagonistic game. The game payoff vector calculated based on the calculations system COMSOL Muliphysics. The solution of this game calculated based on algorithms of multy-swarm multy-agent optimization from sat of Pareto-optimal solutions based on binary preferences relationship.

3. The main advantage of using a electromagnetic hybrid active-passive shield, including an active and a multy-circuit passive part, is the possibility of reducing the level of the initial magnetic field induction in a significantly larger part of the shielding space compared to using only the active shield.

4. During the design of electromagnetic hybrid active-passive shield, the coordinates of the spatial arrangement of 11 circuit passive screens and the coordinates of the spatial location of one compensation winding, as well as the current and phase in this winding of the active shielding system were calculated.

5. The results of the performed theoretical studies what is confirmed byexperimental studies have shown that the shielding factor for only multy-circuit passive shield consisting of 11 aluminum contours with a diameter of 8 mm is about 1.2 units, for only active shield made in the form of a winding consisting of 20 turns is about 4 units and for electromagnetic hybrid active-passive shield, the shielding factor is more 6.2 units, what is confirmed by theoretical and experimental studies.

6. The practical use of the developed electromagnetic hybrid active-passive shield will allow to reduce the level of the magnetic field in a residential building from a double-circuit power transmission line with a «barrel» type arrangement of wires to a safe level for the population of 0.5 μT.

Acknowledgments. The authors express their gratitude to the engineers Sokol A.V. and Shevchenko A.P. of the Department of Magnetism of Technical Objects of Anatolii Pidhornyi Institute of Mechanical Engineering Problems of the National Academy of Sciences of Ukraine for the creative approach and courage shown during the creation under fire, under martial law, of an experimental installation and successful testing of a laboratory model of the system of active silencing.

Conflict of interest. The authors declare that they have no conflicts of interest.

REFERENCES

1. Sung H., Ferlay J., Siegel R.L., Laversanne M., Soerjomataram I., Jemal A., Bray, F. Global Cancer Statistics 2020: GLOBOCAN Estimates of Incidence and Mortality Worldwide for 36 Cancers in 185 Countries. *CA: A Cancer Journal for Clinicians*, 2021, vol. 71, no. 3, pp. 209-249. doi: https://doi.org/10.3322/caac.21660.

2. Directive 2013/35/EU of the European Parliament and of the Council of 26 June 2013 on the minimum health and safety requirements regarding the exposure of workers to the risks arising from physical agents (electromagnetic fields). Available at: http://data.europa.eu/eli/dir/2013/35/oj (Accessed 25.04.2024).

3. *The International EMF Project. Radiation & Environmental Health Protection of the Human Environment World Health Organization*. Geneva, Switzerland, 1996. 2 p. Available at: https://www.who.int/initiatives/the-international-emf-project (Accessed 25.04.2024).
4. Rozov V., Grinchenko V., Tkachenko O., Yerisov A. Analytical Calculation of Magnetic Field Shielding Factor for Cable Line with Two-Point Bonded Shields. *2018 IEEE 17th International Conference on Mathematical Methods in Electromagnetic Theory (MMET)*, 2018, pp. 358-361. doi: https://doi.org/10.1109/MMET.2018.8460425.
5. Rozov V.Yu., Reutskyi S.Yu., Pelevin D.Ye., Kundius K.D. Approximate method for calculating the magnetic field of 330-750 kV high-voltage power line in maintenance area under voltage. *Electrical Engineering & Electromechanics*, 2022, no. 5, pp. 71-77. doi: https://doi.org/10.20998/2074-272X.2022.5.12.
6. Rozov V.Y., Pelevin D.Y., Levina S.V. Experimental research into indoor static geomagnetic field weakening phenomenon. *Electrical Engineering & Electromechanics*, 2013, no. 6, pp. 72-76. (Rus).
7. Rozov V.Y., Kvytsynskyi A.A., Dobrodeyev P.N., Grinchenko V.S., Erisov A.V., Tkachenko A.O. Study of the magnetic field of three phase lines of single core power cables with two-end bonding of their shields. *Electrical Engineering & Electromechanics*, 2015, no. 4, pp. 56-61. (Rus). doi: https://doi.org/10.20998/2074-272X.2015.4.11.
8. Salceanu A., Paulet M., Alistar B.D., Asiminicesei O. Upon the contribution of image currents on the magnetic fields generated by overhead power lines. *2019 International Conference on Electromechanical and Energy Systems (SIELMEN).* 2019. doi: https://doi.org/10.1109/sielmen.2019.8905880.
9. Del Pino Lopez J.C., Romero P.C. Influence of different types of magnetic shields on the thermal behavior and ampacity of underground power cables. *IEEE Transactions on Power Delivery*, Oct. 2011, vol. 26, no. 4, pp. 2659-2667. doi: https://doi.org/10.1109/tpwrd.2011.2158593.
10. Hasan G.T., Mutlaq A.H., Ali K.J. The Influence of the Mixed Electric Line Poles on the Distribution of Magnetic Field. *Indonesian Journal of Electrical Engineering and Informatics (IJEEI)*, 2022, vol. 10, no. 2, pp. 292-301. doi: https://doi.org/10.52549/ijeei.v10i2.3572.
11. Victoria Mary S., Pugazhendhi Sugumaran C. Investigation on magneto-thermal-structural coupled field effect of nano coated 230 kV busbar. *Physica Scripta*, 2020, vol. 95, no. 4, art. no. 045703. doi: https://doi.org/10.1088/1402-4896/ab6524.
12. Ippolito L., Siano P. Using multi-objective optimal power flow for reducing magnetic fields from power lines. *Electric Power Systems Research*, 2004, vol. 68, no. 2, pp. 93-101. doi: https://doi.org/10.1016/S0378-7796(03)00151-2.
13. Barsali S., Giglioli R., Poli D. Active shielding of overhead line magnetic field: Design and applications. *Electric Power Systems Research*, May 2014, vol. 110, pp. 55-63. doi: https://doi.org/10.1016/j.epsr.2014.01.005.
14. Bavastro D., Canova A., Freschi F., Giaccone L., Manca M. Magnetic field mitigation at power frequency: design principles and case studies. *IEEE Transactions on Industry Applications*, May 2015, vol. 51, no. 3, pp. 2009-2016. doi: https://doi.org/10.1109/tia.2014.2369813.
15. Beltran H., Fuster V., García M. Magnetic field reduction screening system for a magnetic field source used in industrial applications. *9 Congreso Hispano Luso de Ingeniería Eléctrica (9 CHLIE)*, Marbella (Málaga, Spain), 2005, pp. 84-99.
16. Bravo-Rodríguez J., Del-Pino-López J., Cruz-Romero P. A Survey on Optimization Techniques Applied to Magnetic Field Mitigation in Power Systems. *Energies*, 2019, vol. 12, no. 7, p. 1332. doi: https://doi.org/10.3390/en12071332.
17. Canova A., del-Pino-López J.C., Giaccone L., Manca M. Active Shielding System for ELF Magnetic Fields. *IEEE Transactions on Magnetics*, March 2015, vol. 51, no. 3, pp. 1-4. doi: https://doi.org/10.1109/tmag.2014.2354515.
18. Canova A., Giaccone L. Real-time optimization of active loops for the magnetic field minimization. *International Journal of Applied Electromagnetics and Mechanics*, Feb. 2018, vol. 56, pp. 97-106. doi: https://doi.org/10.3233/jae-172286.
19. Canova A., Giaccone L., Cirimele V. Active and passive shield for aerial power lines. *Proc. of the 25th International Conference on Electricity Distribution (CIRED 2019)*, 3-6 June 2019, Madrid, Spain. Paper no. 1096.
20. Canova A., Giaccone L. High-performance magnetic shielding solution for extremely low frequency (ELF) sources. *CIRED - Open Access Proceedings Journal*, Oct. 2017, vol. 2017, no. 1, pp. 686-690. doi: https://doi.org/10.1049/oap-cired.2017.1029.
21. Grinchenko V.S., Chunikhin K.V. Magnetic field normalization in residential building located near overhead line by grid shield. *Electrical Engineering & Electromechanics*, 2020, no. 5, pp. 38-43. doi: https://doi.org/10.20998/2074-272X.2020.5.06.
22. Chunikhin K.V., Grinchenko V.S. Normalization of double-circuit overhead line magnetic field inside Khrushchev building. *Electrical Engineering & Electromechanics*, 2021, no. 3, pp. 38-41. doi: https://doi.org/10.20998/2074-272X.2021.3.06.
23. Celozzi S. Active compensation and partial shields for the power-frequency magnetic field reduction. *2002 IEEE International Symposium on Electromagnetic Compatibility*, Minneapolis, MN, USA, 2002, vol. 1, pp. 222-226. doi: https://doi.org/10.1109/isemc.2002.1032478.
24. Celozzi S., Garzia F. Active shielding for power-frequency magnetic field reduction using genetic algorithms optimization. *IEE Proceedings - Science, Measurement and Technology*, 2004, vol. 151, no. 1, pp. 2-7. doi: https://doi.org/10.1049/ip-smt:20040002.
25. Celozzi S., Garzia F. Magnetic field reduction by means of active shielding techniques. *WIT Transactions on Biomedicine and Health*, 2003, vol. 7, pp. 79-89. doi: https://doi.org/10.2495/ehr030091.
26. Popov A., Tserne E., Volosyuk V., Zhyla S., Pavlikov V., Ruzhentsev N., Dergachov K., Havrylenko O., Shmatko O., Averyanova Y., Ostroumov I., Kuzmenko N., Sushchenko O., Zaliskyi M., Solomentsev O., Kuznetsov B., Nikitina T. Invariant Polarization Signatures for Recognition of Hydrometeors by Airborne Weather Radars. *Computational Science and Its Applications – ICCSA 2023. Lecture Notes in Computer Science*, 2023, vol. 13956, pp. 201-217. doi: https://doi.org/10.1007/978-3-031-36805-9_14.
27. Sushchenko O., Averyanova Y., Ostroumov I., Kuzmenko N., Zaliskyi M., Solomentsev O., Kuznetsov B., Nikitina T., Havrylenko O., Popov A., Volosyuk V., Shmatko O., Ruzhentsev N., Zhyla S., Pavlikov V., Dergachov K., Tserne E. Algorithms for Design of Robust Stabilization Systems. *Computational Science and Its Applications – ICCSA 2022. ICCSA 2022. Lecture Notes in Computer Science*, 2022, vol. 13375, pp. 198-213. doi: https://doi.org/10.1007/978-3-031-10522-7_15.
28. Ostroverkhov M., Chumack V., Monakhov E., Ponomarev A. Hybrid Excited Synchronous Generator for Microhydropower Unit. *2019 IEEE 6th International Conference on Energy Smart Systems (ESS)*, Kyiv, Ukraine, 2019, pp. 219-222. doi: https://doi.org/10.1109/ess.2019.8764202.
29. Ostroverkhov M., Chumack V., Monakhov E. Ouput Voltage Stabilization Process Simulation in Generator with Hybrid Excitation at Variable Drive Speed. *2019 IEEE 2nd Ukraine Conference on Electrical and Computer Engineering (UKRCON)*, Lviv, Ukraine, 2019, pp. 310-313. doi: https://doi.org/10.1109/ukrcon.2019.8879781.
30. Tytiuk V., Chornyi O., Baranovskaya M., Serhiienko S., Zachepa I., Tsvirkun L., Kuznetsov V., Tryputen N. Synthesis of a fractional-order $PI^{\lambda}D^{\mu}$-controller for a closed system of switched reluctance motor control. *Eastern-European Journal of Enterprise Technologies*, 2019, no. 2 (98), pp. 35-42. doi: https://doi.org/10.15587/1729-4061.2019.160946.
31. Zagirnyak M., Chornyi O., Zachepa I. The autonomous sources of energy supply for the liquidation of technogenic accidents. *Przeglad Elektrotechniczny*, 2019, no. 5, pp. 47-50. doi: https://doi.org/10.15199/48.2019.05.12.
32. Chornyi O., Serhiienko S. A virtual complex with the parametric adjustment to electromechanical system parameters. *Technical Electrodynamics*, 2019, no. 1, pp. 38-41. doi: https://doi.org/10.15407/techned2019.01.038.
33. Shchur I., Kasha L., Bukavyn M. Efficiency Evaluation of Single and Modular Cascade Machines Operation in Electric Vehicle. *2020 IEEE 15th International Conference on Advanced Trends in Radioelectronics, Telecommunications and Computer Engineering (TCSET)*, Lviv-Slavske, Ukraine, 2020, pp. 156-161. doi: https://doi.org/10.1109/tcset49122.2020.235413.
34. Zhyla S., Volosyuk V., Pavlikov V., Ruzhentsev N., Tserne E., Popov A., Shmatko O., Havrylenko O., Kuzmenko N., Dergachov K., Averyanova Y., Sushchenko O., Zaliskyi M., Solomentsev O., Ostroumov I., Kuznetsov B., Nikitina T. Practical imaging algorithms in ultra-wideband radar systems using active aperture synthesis and

stochastic probing signals. *Radioelectronic and Computer Systems*, 2023, no. 1, pp. 55-76. doi: https://doi.org/10.32620/reks.2023.1.05.
35. Havrylenko O., Dergachov K., Pavlikov V., Zhyla S., Shmatko O., Ruzhentsev N., Popov A., Volosyuk V., Tserne E., Zaliskyi M., Solomentsev O., Ostroumov I., Sushchenko O., Averyanova Y., Kuzmenko N., Nikitina T., Kuznetsov B. Decision Support System Based on the ELECTRE Method. *Data Science and Security. Lecture Notes in Networks and Systems*, 2022, vol. 462, pp. 295-304. doi: https://doi.org/10.1007/978-981-19-2211-4_26.
36. Solomentsev O., Zaliskyi M., Averyanova Y., Ostroumov I., Kuzmenko N., Sushchenko O., Kuznetsov B., Nikitina T., Tserne E., Pavlikov V., Zhyla S., Dergachov K., Havrylenko O., Popov A., Volosyuk V., Ruzhentsev N., Shmatko O. Method of Optimal Threshold Calculation in Case of Radio Equipment Maintenance. *Data Science and Security. Lecture Notes in Networks and Systems*, 2022, vol. 462, pp. 69-79. doi: https://doi.org/10.1007/978-981-19-2211-4_6.
37. Shmatko O., Volosyuk V., Zhyla S., Pavlikov V., Ruzhentsev N., Tserne E., Popov A., Ostroumov I., Kuzmenko N., Dergachov K., Sushchenko O., Averyanova Y., Zaliskyi M., Solomentsev O., Havrylenko O., Kuznetsov B., Nikitina T. Synthesis of the optimal algorithm and structure of contactless optical device for estimating the parameters of statistically uneven surfaces. *Radioelectronic and Computer Systems*, 2021, no. 4, pp. 199-213. doi: https://doi.org/10.32620/reks.2021.4.16.
38. Volosyuk V., Zhyla S., Pavlikov V., Ruzhentsev N., Tserne E., Popov A., Shmatko O., Dergachov K., Havrylenko O., Ostroumov I., Kuzmenko N., Sushchenko O., Averyanova Yu., Zaliskyi M., Solomentsev O., Kuznetsov B., Nikitina T. Optimal Method for Polarization Selection of Stationary Objects Against the Background of the Earth's Surface. *International Journal of Electronics and Telecommunications*, 2022, vol. 68, no. 1, pp. 83-89. doi: https://doi.org/10.24425/ijet.2022.139852.
39. Halchenko V., Trembovetska R., Bazilo C., Tychkova N. Computer Simulation of the Process of Profiles Measuring of Objects Electrophysical Parameters by Surface Eddy Current Probes. *Lecture Notes on Data Engineering and Communications Technologies*, 2023, vol. 178, pp. 411-424. doi https://doi.org/10.1007/978-3-031-35467-0_25.
40. Halchenko V., Bacherikov D., Filimonov S., Filimonova N. Improvement of a Linear Screw Piezo Motor Design for Use in Accurate Liquid Dosing Assembly. *Smart Technologies in Urban Engineering. STUE 2022. Lecture Notes in Networks and Systems*, 2023, vol. 536, pp. 237-247. doi: https://doi.org/10.1007/978-3-031-20141-7_22.
41. Ruzhentsev N., Zhyla S., Pavlikov V., Volosyuk V., Tserne E., Popov A., Shmatko O., Ostroumov I., Kuzmenko N., Dergachov K., Sushchenko O., Averyanova Y., Zaliskyi M., Solomentsev O., Havrylenko O., Kuznetsov B., Nikitina T. Radio-Heat Contrasts of UAVs and Their Weather Variability at 12 GHz, 20 GHz, 34 GHz, and 94 GHz Frequencies. *ECTI Transactions on Electrical Engineering, Electronics, and Communications*, 2022, vol. 20, no. 2, pp. 163-173. doi: https://doi.org/10.37936/ecti-eec.2022202.246878.
42. Maksymenko-Sheiko K.V., Sheiko T.I., Lisin D.O., Petrenko N.D. Mathematical and Computer Modeling of the Forms of Multi-Zone Fuel Elements with Plates. *Journal of Mechanical Engineering*, 2022, vol. 25, no. 4, pp. 32-38. doi: https://doi.org/10.15407/pmach2022.04.032.
43. Hontarovskyi P.P., Smetankina N.V., Ugrimov S.V., Garmash N.H., Melezhyk I.I. Computational Studies of the Thermal Stress State of Multilayer Glazing with Electric Heating. *Journal of Mechanical Engineering*, 2022, vol. 25, no. 1, pp. 14-21. doi: https://doi.org/10.15407/pmach2022.02.014.
44. Kostikov A.O., Zevin L.I., Krol H.H., Vorontsova A.L. The Optimal Correcting the Power Value of a Nuclear Power Plant Power Unit Reactor in the Event of Equipment Failures. *Journal of Mechanical Engineering*, 2022, vol. 25, no. 3, pp. 40-45. doi: https://doi.org/10.15407/pmach2022.03.040.
45. Rusanov A.V., Subotin V.H., Khoryev O.M., Bykov Y.A., Korotaiev P.O., Ahibalov Y.S. Effect of 3D Shape of Pump-Turbine Runner Blade on Flow Characteristics in Turbine Mode. *Journal of Mechanical Engineering*, 2022, vol. 25, no. 4, pp. 6-14. doi: https://doi.org/10.15407/pmach2022.04.006.
46. Ummels M. *Stochastic Multiplayer Games Theory and Algorithms*. Amsterdam University Press, 2010. 174 p.
47. Ray T., Liew K.M. A Swarm Metaphor for Multiobjective Design Optimization. *Engineering Optimization*, 2002, vol. 34, no. 2, pp. 141-153. doi: https://doi.org/10.1080/03052150210915.
48. Xiaohui Hu, Eberhart R.C., Yuhui Shi. Particle swarm with extended memory for multiobjective optimization. *Proceedings of the 2003 IEEE Swarm Intelligence Symposium*. SIS'03 (Cat. No.03EX706), Indianapolis, IN, USA, 2003, pp. 193-197. doi: https://doi.org/10.1109/sis.2003.1202267.
49. Dergachov K., Havrylenko O., Pavlikov V., Zhyla S., Tserne E., Volosyuk V., Ruzhentsev N., Ostroumov I., Averyanova Y., Sushchenko O., Popov A., Shmatko O., Solomentsev O., Zaliskyi M., Kuzmenko N., Kuznetsov B., Nikitina T. GPS Usage Analysis for Angular Orientation Practical Tasks Solving. *2022 IEEE 9th International Conference on Problems of Infocommunications, Science and Technology (PIC S&T)*, 2022, pp. 187-192. doi: https://doi.org/10.1109/PICST57299.2022.10238629.
50. Zhyla S., Volosyuk V., Pavlikov V., Ruzhentsev N., Tserne E., Popov A., Shmatko O., Havrylenko O., Kuzmenko N., Dergachov K., Averyanova Y., Sushchenko O., Zaliskyi M., Solomentsev O., Ostroumov I., Kuznetsov B., Nikitina T. Statistical synthesis of aerospace radars structure with optimal spatio-temporal signal processing, extended observation area and high spatial resolution. *Radioelectronic and Computer Systems*, 2022, no. 1, pp. 178-194. doi: https://doi.org/10.32620/reks.2022.1.14.
51. Hashim F.A., Hussain K., Houssein E.H., Mabrouk M.S., Al-Atabany W. Archimedes optimization algorithm: a new metaheuristic algorithm for solving optimization problems. *Applied Intelligence*, 2021, vol. 51, no. 3, pp. 1531-1551. doi: https://doi.org/10.1007/s10489-020-01893-z.

Received 14.01.2024
Accepted 13.03.2024
Published 20.06.2024

B.I. Kuznetsov[1], *Doctor of Technical Science, Professor,*
T.B. Nikitina[2], *Doctor of Technical Science, Professor,*
I.V. Bovdui[1], *PhD, Senior Research Scientist,*
K.V. Chunikhin[1], *PhD, Senior Research Scientist,*
V.V. Kolomiets[2], *PhD, Assistant Professor,*
B.B. Kobylianskyi[2], *PhD, Assistant Professor,*
[1] Anatolii Pidhornyi Institute of Mechanical Engineering Problems of the National Academy of Sciences of Ukraine,
2/10, Pozharskogo Str., Kharkiv, 61046, Ukraine,
e-mail: kuznetsov.boris.i@gmail.com (Corresponding Author)
[2] Educational Scientific Professional Pedagogical Institute V.N. Karazin Kharkiv National Univesity,
9a, Nosakov Str., Bakhmut, Donetsk Region, 84511, Ukraine,
e-mail: nnppiuipa@ukr.net

How to cite this article:
Kuznetsov B.I., Nikitina T.B., Bovdui I.V., Chunikhin K.V., Kolomiets V.V., Kobylianskyi B.B. The method for design of electromagnetic hybrid active-passive shielding by overhead power lines magnetic field. *Electrical Engineering & Electromechanics*, 2024, no. 4, pp. 22-30. doi: https://doi.org/10.20998/2074-272X.2024.4.03